Evaluation of The Effect of Outer Skin Slope on Fire Safety in Double-Skin Façade Systems

Mehmet Akif Yıldız[1*] (iD), Figen Beyhan[2] (iD)

[1] Ministry of Environment Urbanization and Climate Change, Ankara, Türkiye, makif.yildiz@csb.gov.tr
[2] Gazi University, Faculty of Science, Department of Architecture, Ankara, Türkiye, fbeyhan@gazi.edu.tr
*Corresponding Author

ARTICLE INFO	ABSTRACT
Keywords: Double Skin Façede Outer Skin Slope Fire Safety Smoke Spread Computational Fluid Dynamic Article History: Received: 13.10.2023 Accepted: 24.11.2023 Online Available:27.02.2024	In order to increase energy efficiency and user comfort, double skin façade designs are becoming increasingly popular in the built environment as an alternative to traditional façede and curtain walling systems. The vertical cavity between the outer and inner skins of double skin façade systems, which is critical for natural ventilation, can destroy the effectiveness of façade designs by creating fire hazards due to the creation of uninterrupted areas between spaces. It is essential for the sustainability of the buildings to make appropriate fire safety designs for the risks of spreading toxic gases released in a possible fire through the double skin façede cavity to monitor the design before the building is built and to take the necessary precautions. Therefore, that paper developed a numerical model using computational fluid dynamics to monitor the smoke propagation through the cavity of the double skin façade and the temperature changes in the building. As a contribution to the physical modeling studies of double skin façade systems in the literature, the effect of changing the slope of the outer skin on smoke propagation and temperature changes was investigated. A design model was created by developing 9 scenarios: 4 wide angles, 4 acute angles, and a right angle, each with an angle varying by 3 degrees. While acute-angle cavity designs increased the flue effect in the cavity and increased the direction speed and density of the smoke towards the cavity, wide-angle cavity designs reduced the ambient temperature.

1. Introduction

The energy and economic crises emerging in the globalizing world have affected the building design and the effect of developing technology, the building envelope has gone beyond being a cover separating the interior and exterior spaces and has become a building element that improves building performance. Thus, in addition to aesthetic concerns, the shell has turned into a design element that provides energy conservation and healthy living spaces by allowing climatic elements to be taken into the interior space in a controlled manner. Double skin façade systems, which have developed as an alternative to traditional and single-layer curtain wall systems, have been preferred in built environments in recent years because they allow

controlled intake of climatic data such as wind, sun, humidity, and external pressure. Double skin façade systems consist of an outer skin, an inner skin, and the air cavity between these two layers. In double skin façade systems, the outer skin protects the building from adverse environmental conditions and provides control of natural ventilation with the help of vents on it. These vents provide air to be drawn into the cavity and, thanks to the open windows, allow natural, fresh air to enter the interior. In the inner layer, window can be opened as desired with the opportunity given by the outer layer. However, as this façade system creates uninterrupted areas between internal spaces through vertical and horizontal cavities, it poses fire risks if the necessary measures are not taken.

Predicting the development and hazards of fires is an excellent opportunity to prevent and extinguish fires in time effectively. In fire safety research, it is inefficient to carry out actual fire testing because the cost of fire testing is high, the experimental environment preparation time is long, and the experiment process has hazards. Therefore, using computer simulation to analyze fire problems is also valuable research. The key point of the computer model is to build a fire model so that the development process of fire can be analyzed and understood without building construction. For the fire model, computational fluid dynamics is widely used, which uses numerical methods and algorithms to analyze and solve fluid mechanics (CFD) and heat transfer problems.

In the physical model studies with CFD, studies examining the fire problems caused by double-skin facades, the resistance of the glass in the outer and inner skin, smoke propagation in the cavity, and the effect of blind elements on fire have been investigated. In recent years, physical model studies of double skin façades have generally investigated the effect on fire of blinds placed in the cavity or glazing of the double skin façade.

It has been demonstrated that the blind angle and position have a significant effect on the fire propagation characteristics and temperature distribution in the double skin façade and should be taken into account [1-3]. The risks posed by smoke and flame clouds moving parallel to the airflow in naturally ventilated double-skin facades were among the research areas numerically analyzed in the literature. In these studies, smoke, temperature, pressure, and flame cloud analyses were carried out with scenarios consisting of the type of double skin façade, cavity width, physical properties of the spaces facing the cavity, position and size of window openings, air inlet, and outlet properties [4-11].

It has been observed that the parameters that affect smoke propagation and temperature in double-shell facades are cavity width and ventilation openings. It has been shown that the decrease in the cavity width increases the chimney effect in the cavity and increases the smoke velocity and temperature in the cavity. It has been shown that the air outlets opening out of the double shell facade cavity are dimensionally larger than the ventilation openings in the spaces, which increases the efficiency of smoke evacuation through the cavity.

In the studies analyzing the performance of the glass of the outer skin and inner skin due to high temperature and pressure in a fire, scenarios were created from the glass's physical and mechanical properties and the cavity's properties [12-16]. Experiments and numerical analyses were carried out to measure the surface temperature and heat flow in the outer and inner glass panes and to investigate the cracking patterns, breakage and collapse of the glass panels. As the cavity width increases, smoke and flame move towards the outer glass, making the inner glass safer. As the cavity width decreased, the temperature inside the cavity increased and cracking and breakage occurred in the glass.

2. Material and Methods

Within the scope of the study, the effect of outer skin geometry on fire propagation in double skin façade cavities was numerically investigated using (CFD). Unlike the physical modeling studies in the literature, this study investigated the effect of the slope of the façade on the spread of smoke and temperature rise in the building due to the fire starting in the spaces adjacent to the double skin façade.

2.1. Prototype building design

Based on the relevant studies in the literature, a prototype building was designed to investigate smoke movement and temperature levels in the double skin cavity, neglecting the effect of climatic elements such as the environment and prevailing wind. Each floor of the three-story prototype building has a 400 x 600 x 350 cm (width x length x height) space with a double-skin façade cavity on one side and an atrium on the other. The working principle of the double skin façade was to provide an air inlet on the lower surface of the outer skin and an air outlet on the upper surface. Air inlets and outlets were designed with dimensions of 350x50 cm, while

100x150 cm window openings and 100x210 cm door openings were placed in the rooms. The cavity width in the double skin façade was designed to be 250 cm, but the cavity width and volume changed as the slope of the outer skin changed. The dimensions of the atrium, which had a 200 x 100 cm ceiling vent, were 350 x 400 x 1050 cm (width x length x height). As the material design is not the subject of the study, the walls, ceilings, and floors of the entire building have been designed as concrete with a thermal inertia $k\rho c$ of approximately 2 kWs /m4 k² (Figure 1).
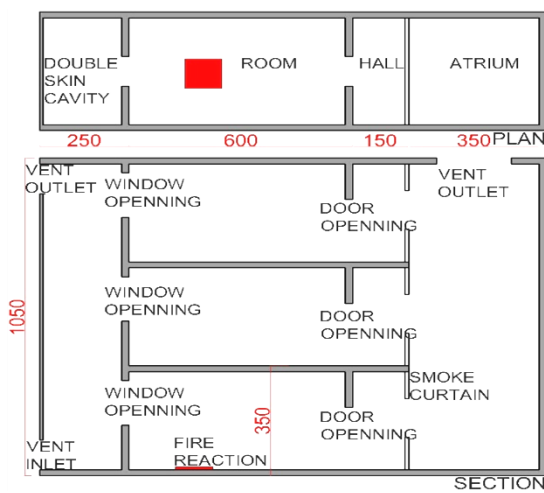
Figure 1. Prototype building plan and section

2.2. Design fire and numerical model features

Studies that provide performance-based approaches through CFD use the t-squared fire model, where the combustion rate varies with the square of time. The curve expressing the ratio of the combustion rate to the square of time for a T-squared fire shows the time required to reach the highest heat release rate. If the heat release rate is known, which gives the most crucial information about how much heat is released when combustible materials burn, temperature, smoke layer thickness, smoke flow rate, and radiant heat flux are also known. The equation giving the heat release rate for a T square fire is given below:

$$Q = \alpha t^p \qquad (1)$$

Q: Heat release rate Btu/s (kW)
α: Fire growth coefficient Btu/s3 (kW/s2)
t: Time from ignition (s)

p: Positive exponent

While the NFPA 92 Smoke Control Systems Standard classifies the fire growth rate as slow, medium, fast, and ultra-fast, it calculates the reference heat release rate as 1055 kW for physical model studies. Figure 2 shows the fire growth curve for slow, medium, fast, and ultra-fast growth rates according to the above equation to reach the reference heat release rate of 1055 kW [19].
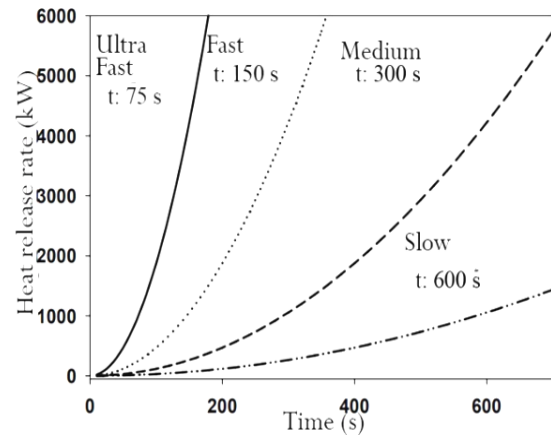

Figure 2. Fire growth rate for the reference heat release rate [20]

According to Figure 2, the time to reach the reference heat release rate was 150 seconds and the fire growth coefficient (α) was calculated as 0.047 kW/s² from Equation 1. The 100 x 100 cm reaction source was selected as polyurethane GM27 consisting of 1.00 carbon, 1.7 hydrogen, 0.3 oxygen and 0.08 nitrogen atoms. For this reaction source, smoke production is 0.198 g/g and carbon monoxide (CO) production is 0.042 g/g. Table 1 shows the features of the design fire [21].

Table 1. Design fire features

Feature	Value
Reaction type	Polyurethane GM27
Fire growth	Fast
Smoke production	0.198 g/g
CO production	0.042 g/g
Heat release rate	1055
Fire growth coefficient	0.047
Ignition start time	10 s
Simulation duration	160 s
Ambient temperature	10 ^{0}C

The study used the Pyrosim program, which includes FDS functions and Smokeview visualization, to create geometry and define boundaries. To create the three-dimensional model in Pyrosim, the lengths of the cell network structure in which the boundaries were determined were set to 0.2x0.2x0.2m. direction to be used for measuring temperature, smoke movement, and velocity, a total of 3 thermocouples, in the double-skin facade cavity, in the atrium cavity, and the last floor room, were placed to measure the temperature (Figure 3).
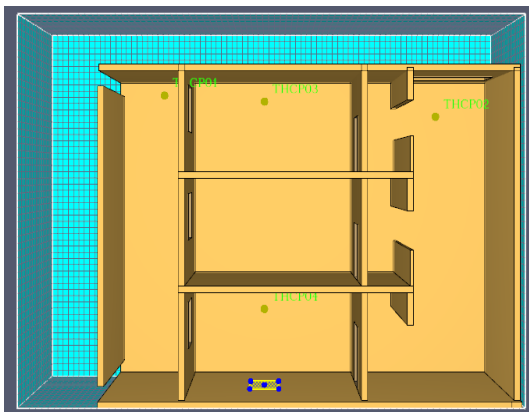
Figure 1. Computer model features

In order to examine the effect of changing the slope of the outer skin of the double-skin facade on fire, a total of 9 scenarios were determined as a result of changing the outer skin slope by 3 degrees, considering that all conditions are constant (Figure 4). As a result of modeling 9 scenarios, numerical analyses were performed, and the findings were discussed in the context of smoke propagation and temperature levels.
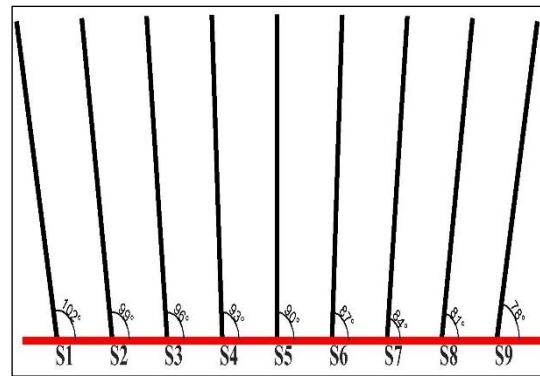

Figure 4. Scenarios with changing the slope of the outer skin of the design model

3. Findings

Based on the design fire' characteristics and prototype building design, the findings of 9 scenarious consisting of outer skin slopes were analysed.

The smoke views during the Scenario 1 simulation process were shown in Figure 5. In the double skin cavity, the smoke reached the first floor window level at 40. seconds and the air outlet in the cavity at 75. seconds. The smoke passed into the atrium cavity at 80 seconds. Smoke also entered the room on the last floor at 72. seconds, and was filled with smoke at 110. seconds.
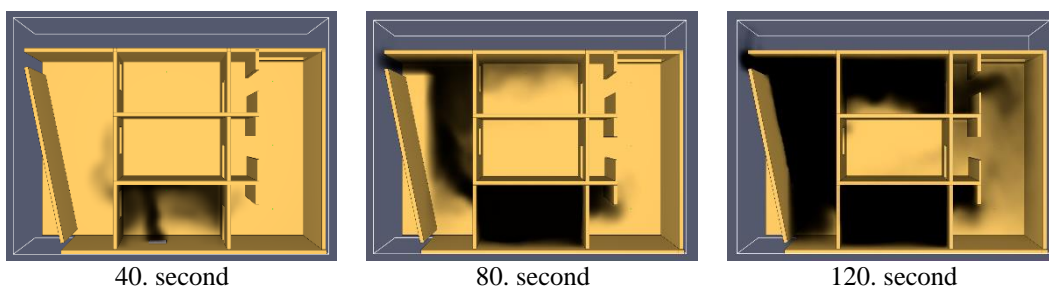

| 40. second | 80. second | 120. second |

Figure 5. Scenario 1 smoke view

In scenario 1, the temperature values measured at the thermocouples were 46.04 ^{0}C at the top floor room, 73.52 ^{0}C at the upper level of the double skin cavity and 27.14 ^{0}C at the upper level of the atrium. The highest ambient temperature during the simulation period was 145.8 ^{0}C (Figure 6).
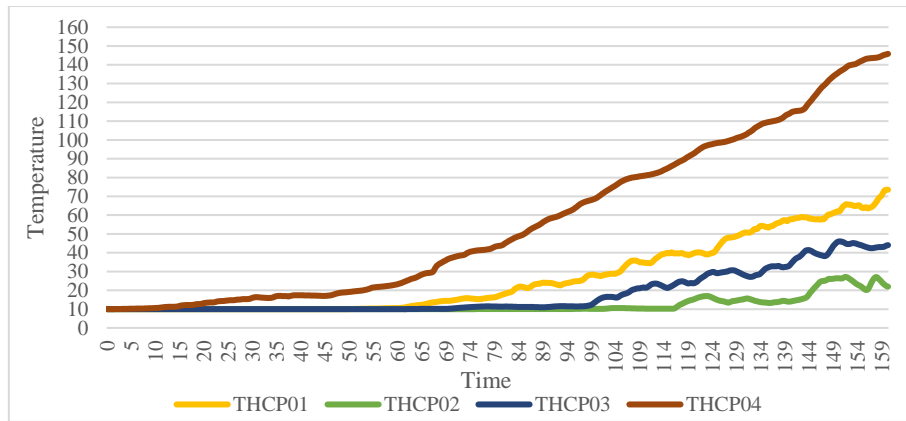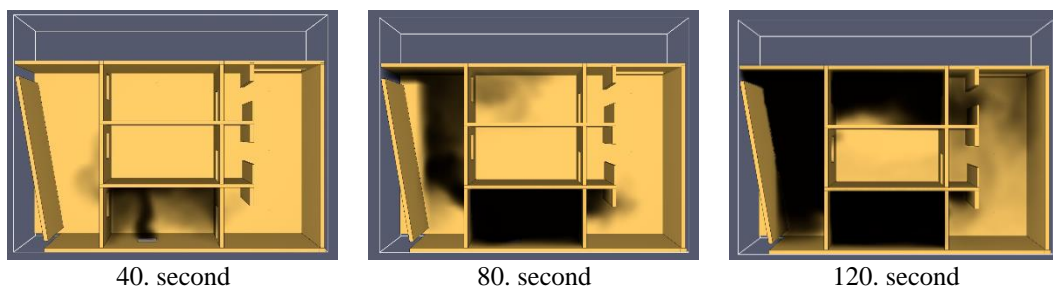
Figure 6. Scenario 1 time dependent -temerature values

The smoke views during the Scenario 2 simulation process were shown in Figure 7. In the double skin cavity, the smoke reached the first floor window level at 40. seconds and the air outlet in the cavity at 72. seconds. The smoke passed into the atrium cavity at 80. seconds. Smoke also entered the room on the last floor at 70. seconds, and was filled with smoke at 110. seconds.

| 40. second | 80. second | 120. second |

Figure 7. Scenario 2 smoke view

In scenario 2, the temperature values measured at the thermocouples were 42.52 ^{0}C at the top floor room, 69.31 ^{0}C at the upper level of the double skin cavity and 27.46 ^{0}C at the upper level of the atrium. The highest ambient temperature during the simulation period was 142.33 ^{0}C (Figure 8).
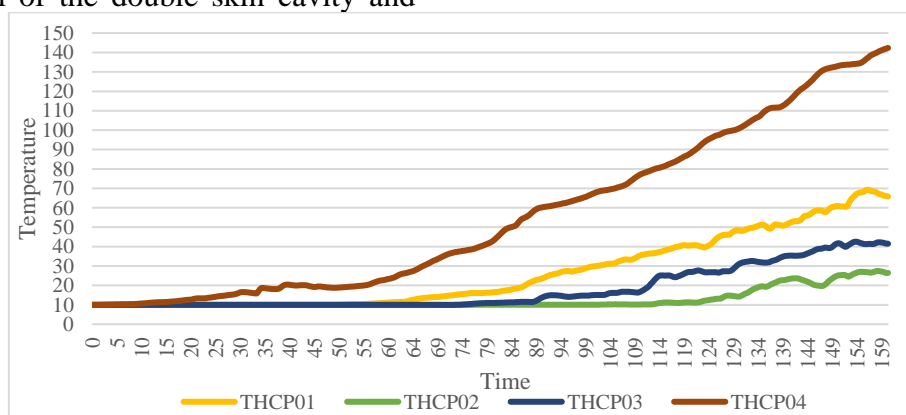

Figure 8. Scenario 2 time-dependent temperature values

The smoke views during the Scenario 3 simulation process were shown in Figure 9. In the double skin cavity, the smoke reached the first floor window level at 40. seconds and the air outlet in the cavity at 70. seconds. The smoke passed into the atrium cavity at 75. seconds. Smoke also entered the room on the

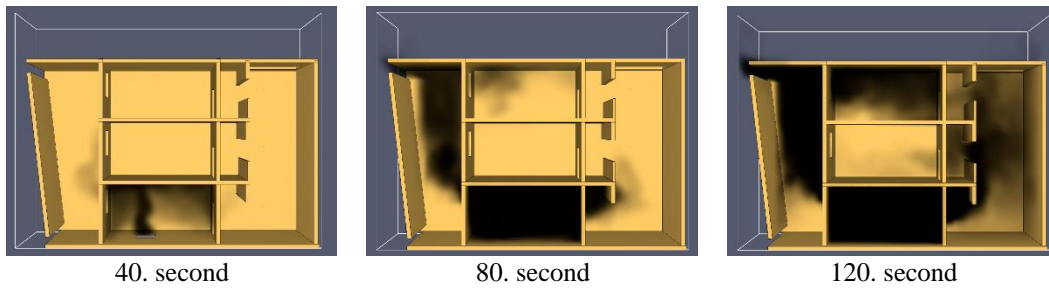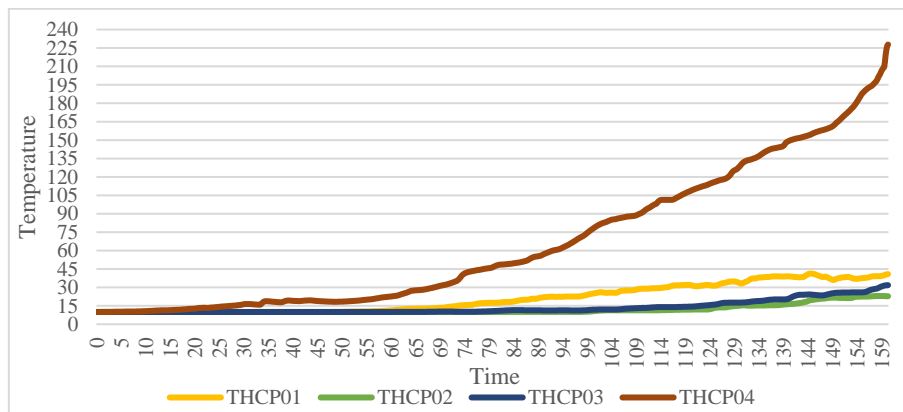last floor at 70. seconds, and was filled with smoke at 115. seconds.

| 40. second | 80. second | 120. second |

Figure 9. Scenario 3 smoke view

In scenario 3, the temperature values measured at the thermocouples were 31.80 ^{0}C at the top floor room, 41.28 ^{0}C at the upper level of the double skin cavity and 22.98 ^{0}C at the upper level of the atrium. The highest ambient temperature during the simulation period was 227.82 ^{0}C (Figure 10).

Figure 10. Scenario 3 time-dependent temperature values

The smoke views during the Scenario 4 simulation process were shown in Figure 11. In the double skin cavity, the smoke reached the first floor window level at 40. seconds and the air outlet in the cavity at 65. seconds. The smoke passed into the atrium cavity at 72. seconds. Smoke also entered the room on the last floor at 68. seconds, and was filled with smoke at 115. seconds.
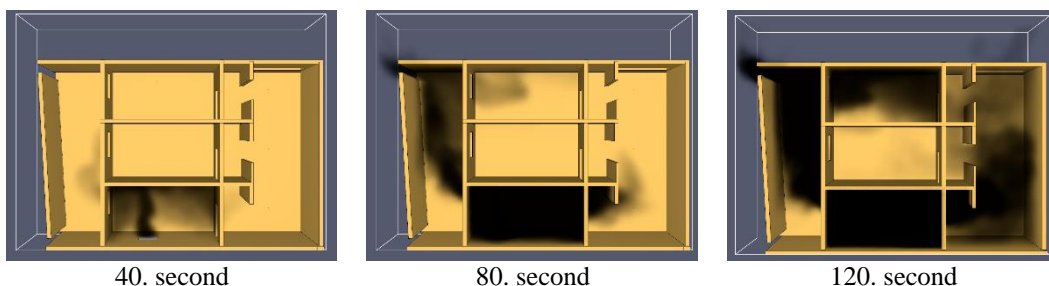

| 40. second | 80. second | 120. second |

Figure 11. Scenario 4 smoke view

In scenario 4, the temperature values measured at the thermocouples were 24.64 ^{0}C at the top floor room, 41.99 ^{0}C at the upper level of the double skin cavity and 27.48 ^{0}C at the upper level of the atrium. The highest

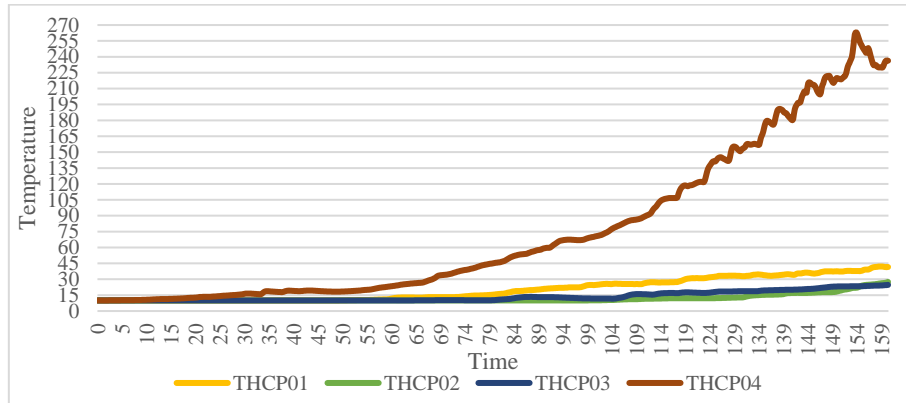ambient temperature during the simulation period was 263.07 ^{0}C (Figure 12).

Figure 12. Scenario 4 time-dependent temperature values

The smoke views during the Scenario 5 simulation process were shown in Figure 13. In the double skin cavity, the smoke reached the first floor window level at 40. seconds and the air outlet in the cavity at 60. seconds. The smoke passed into the atrium cavity at 78. seconds. Smoke also entered the room on the last floor at 70. seconds, and was filled with smoke at 110. seconds.
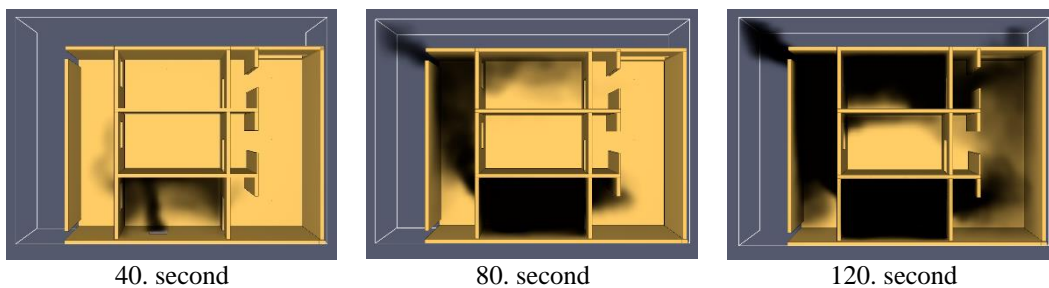

| 40. second | 80. second | 120. second |

Figure 13. Scenario 5 smoke view

In scenario 5, the temperature values measured at the thermocouples were 42.18 ^{0}C at the top floor room, 60.72 ^{0}C at the upper level of the double skin cavity and 26.23 ^{0}C at the upper level of the atrium. The highest ambient temperature during the simulation period was 206.94 ^{0}C (Figure 14).
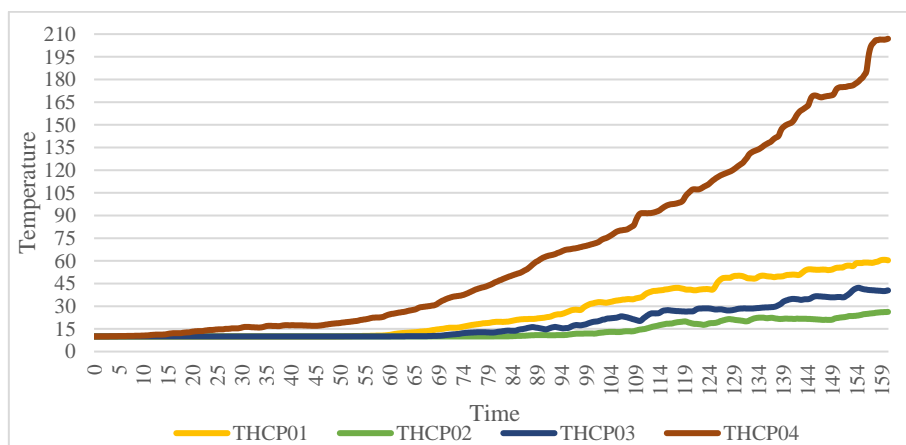

Figure 14. Scenario 5 time dependent temperature values

The smoke views during the Scenario 6 simulation process were shown in Figure 15. In the double skin cavity, the smoke passed the first floor window level at 40. seconds and the air outlet in the cavity at 57. seconds. The smoke passed into the atrium cavity at 80. seconds. Smoke also entered the room on the last floor at 62. seconds, and was filled with smoke at 105. seconds.
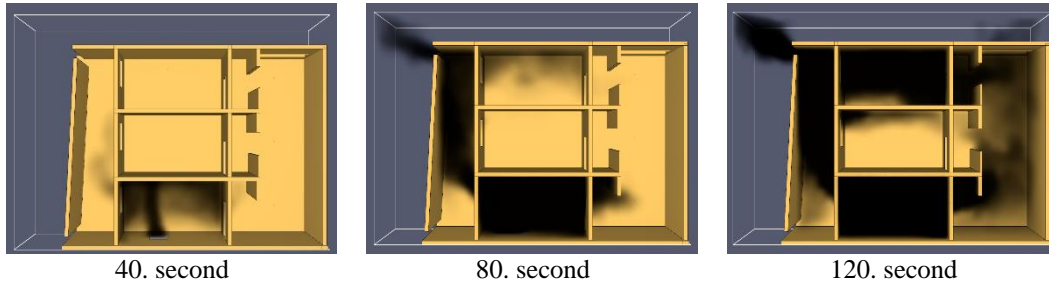

| 40. second | 80. second | 120. second |

Figure 15. Scenario 6 smoke view

In scenario 6, the temperature values measured at the thermocouples were 41.75 ^{0}C at the top floor room, 57.69 ^{0}C at the upper level of the double skin cavity and 27.74 ^{0}C at the upper level of the atrium. The highest ambient temperature during the simulation period was 194.22 ^{0}C (Figure 16).
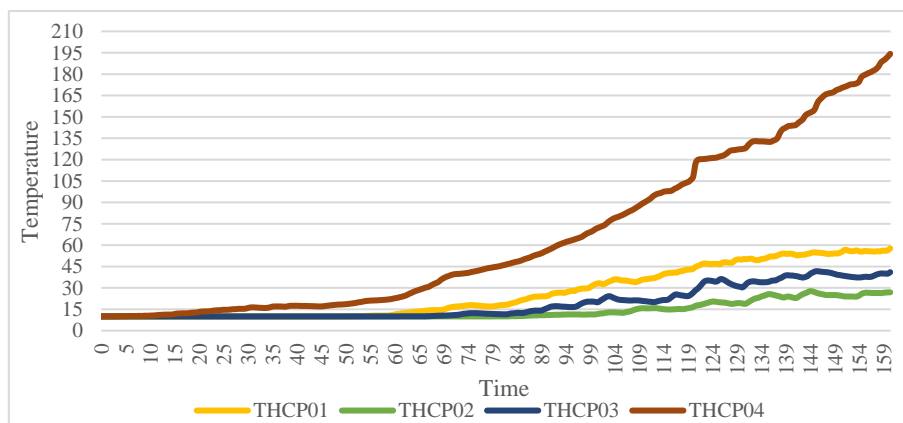

Figure 16. Scenario 6 time dependent temperature value

The smoke views during the Scenario 7 simulation process were shown in Figure 17. In the double skin cavity, the smoke passed the first floor window level at 40. seconds and the air outlet in the cavity at 55. seconds. The smoke passed into the atrium cavity at 80. seconds. Smoke also entered the room on the last floor at 60. seconds, and was filled with smoke at 103. seconds.
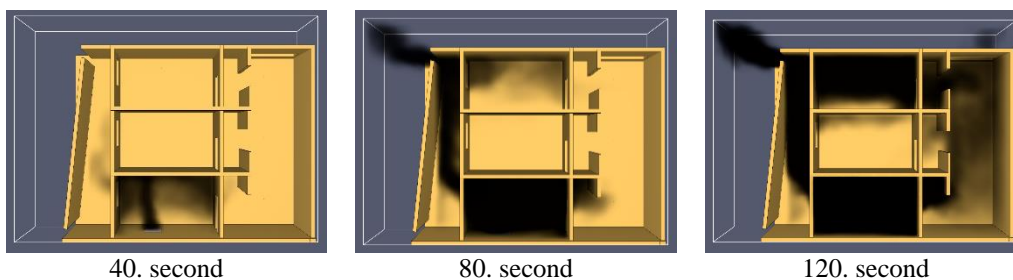

| 40. second | 80. second | 120. second |

Figure 17. Scenario 7 smoke view

In scenario 7, the temperature values measured at the thermocouples were 43.83 ^{0}C at the top floor room, 63.35 ^{0}C at the upper level of the double skin cavity and 26.66 ^{0}C at the upper level of the atrium. The highest ambient temperature during the simulation period was 181.86 ^{0}C (Figure 18).
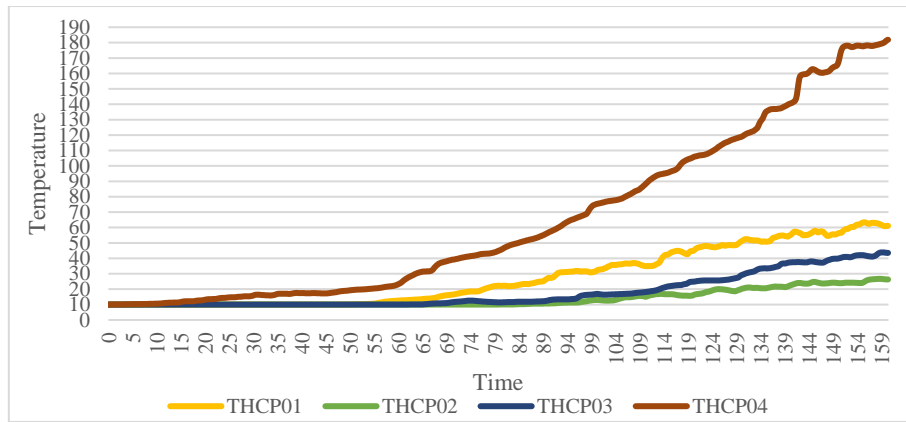

Figure 18. Scenario 7 time dependent temperature values

The smoke views during the Scenario 8 simulation process were shown in Figure 19. In the double skin cavity, the reached the first floor ceiling level at 40. seconds and the air outlet in the cavity at 52. seconds. The smoke passed into the atrium cavity at 83. seconds. Smoke also entered the room on the last floor at 60. seconds, and was filled with smoke at 107. seconds.

| 40. second | 80. second | 120. second |

Figure 19. Scenario 8 smoke view

In scenario 8, the temperature values measured at the thermocouples were 42.68 ^{0}C at the top floor room, 75.14 ^{0}C at the upper level of the double skin cavity and 28.57 ^{0}C at the upper level of the atrium. The highest ambient temperature during the simulation period was 179.57 ^{0}C (Figure 20).

Figure 20. Scenario 8 time dependent temperature values

The smoke views during the Scenario 9 simulation process were shown in Figure 21. In the double skin cavity, the reached the first floor ceiling level at 40. seconds and the air outlet in the cavity at 50. seconds. The smoke passed into the atrium cavity at 88. seconds. Smoke also entered the room on the last floor at 60. seconds, and was filled with smoke at 120. seconds.
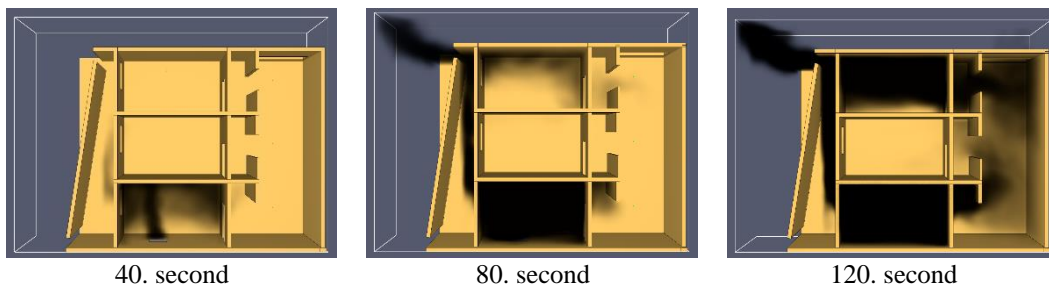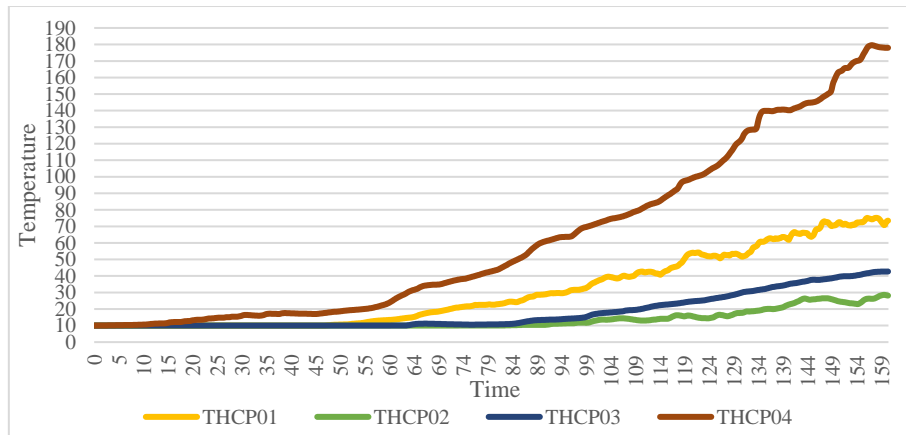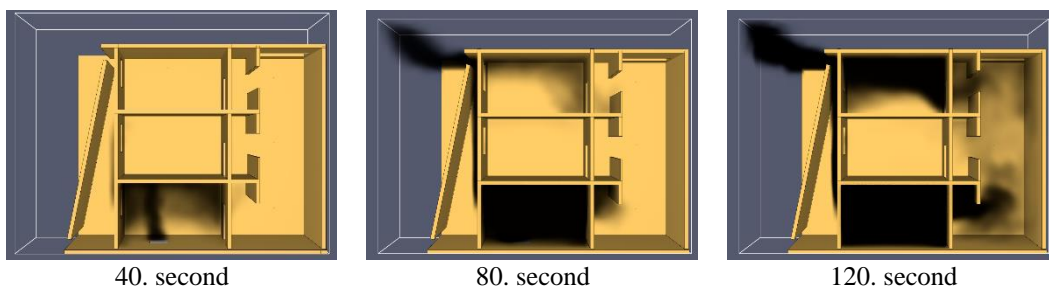

| 40. second | 80. second | 120. second |

Figure 21. Scenario 9 smoke view

In scenario 9, the temperature values measured at the thermocouples were 36.78 ^{0}C at the top floor room, 80.42 ^{0}C at the upper level of the double skin cavity and 18.89 ^{0}C at the upper level of the atrium. The highest ambient temperature during the simulation period was 193.62 ^{0}C (Figure 22).
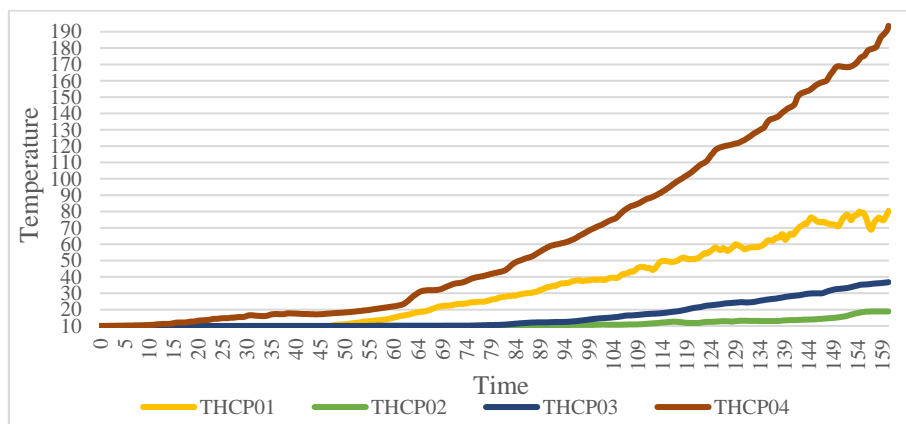

Figure 22. Scenario 9 time dependent temperature values

4. Discussion and Conclusion

The academic studies on double skin façade systems in the literature analyzed numerical models of cavity dimensional properties, ventilation conditions properties, construction, and glass material properties. As a contribution to the literature physical model studies, the effect of the outer shell slope of the double skin façade on smoke extraction and indoor temperature was investigated in this study. In a naturally ventilated double skin façade system, it was observed that changing the slope of the façade by designing the ventilation conditions in the same way in all scenarios significantly affects the smoke extraction from the cavity air outlet and indoor temperature values.

As a result of the cavity slope decreasing and being designed in an upward narrowing structure, the time for the smoke to reach the outside air outlet decreased, and the smoke density in the cavity increased. The smoke filling time in the last floor space was longer in the wide angle cavity designs than in the acute angle cavity designs. Exceptionally, in the S9 scenario, smoke diffusion decreased in areas other than the last cavity due to the high chimney effect in the cavity.

When the slope of the outer shell was increased, and the cavity volume increased by expanding the cavity upwards, the level of smoke in the atrium has decreased compared to the scenario of the right-angled outer shell. Similarly, the smoke density in the atrium decreased in the scenarios with an outer shell inclination of less than 90^0 compared to the right-angled shell scenario. Still, the smoke density has been higher than the wide-angle scenarios. As a result, an outer or inner sloping shell design instead of a right-angled shell design provided the appropriate design criteria for reducing the spread of smoke into the spaces.

While the ambient temperature decreased in the wide-angle scenarios S1 and S2, the highest ambient temperature of 263.07 ^{0}C was reached in the S4 scenario. In the other scenarios, a similar time-dependent temperature increase curve was observed, and in general, a negative correlation

was observed, where the temperature increased as the angle decreased.

According to the temperatures measured from the thermocouple in the last floor room, as the slope angle decreased, the temperature decreased compared to the right-angle scenario, and the temperature was measured 36.79 ^{0}C in the S9 scenario, where the slope was the lowest. As the slope angle increased, the temperature has decreased significantly in the first place, but as the width increased more, the temperature level has reached the same level as the right angle. In the S4 scenario with 93^0 slope, the temperature measured in the last floor room has been the lowest among the scenarios, with 24.64 ^{0}C. This model showed no correlation between the inclination angle and the temperature levels in the last floor room, and a shell inclination increasing by 3 degrees showed the most favorable temperature level at the last floor room.

Since the chimney effect increases as the temperature rises due to the increase in pressure, one of the methods used to determine the strength of the chimney effect in the cavity of the double-skin façade is to measure the temperature levels in the cavity. While the temperature level in the cavity increased in the acute slope skin scenarios, the chimney effect increased as the angle decreased. However, while no negative or positive correlation was observed for the chimney effect temperature relationship for the wide-angle outer shell designs, the cavity temperature was lowest value for the S3 and S4 scenarios compared to the other scenarios.

In this study, the effect of the slope of the outer surface of the double-shell façade on smoke propagation and temperature was investigated, and appropriate cavity design criteria for fire safety were put forward. In addition to ensuring that climatic data can be efficiently taken indoors with appropriate cavity design, smoke extraction can be done through the cavity in case of a fire.

The smoke and other gases generated in the fire will be extracted through the cavity with appropriate cavity designs, and the temperature and smoke levels in other areas of the building will be provided in suitable conditions for evacuating people. Only the effect of the slope of

the outer skin on the fire safety design has been investigated, and it is considered that other design criteria, such as natural ventilation conditions and space dimensions, can be examined by further academic research.

Article Information Form

Authors' Contribution
The authors contributed equally to the study.

The Declaration of Conflict of Interest/ Common Interest
No conflict of interest or common interest has been declared by the authors.

The Declaration of Ethics Committee Approval
This study does not require ethics committee permission or any special permission.

The Declaration of Research and Publication Ethics
The authors of the paper declare that they comply with the scientific, ethical and quotation rules of SAUJS in all processes of the paper and that they do not make any falsification on the data collected. In addition, they declare that Sakarya University Journal of Science and its editorial board have no responsibility for any ethical violations that may be encountered, and that this study has not been evaluated in any academic publication environment other than Sakarya University Journal of Science.

References

[1] D. A. Abdoh, V. K. R. Kodur, K. M. Liew, "Smoothed particle hydrodynamics modeling of the thermal behavior of double skin facades in fires considering the effects of venetian blinds," Applied Mathematical Modelling, vol. 84, pp. 357-376, 2020.

[2] Y. Huang, S. Yeboah, J. Shoa, "Numerical data on fire in the cavity of naturally ventilated double skin façade with venetian blinds," Data in Brief, vol. 46, pp. 108859-108863, 2023a.

[3] Y. Huang, S. Yeboah, J. Shoa, "Numerical investigation of fire in the cavity of naturally ventilated double skin façade with venetian blinds," Building Services Engineering Research and Technology, vol. 44, pp. 45-61, 2023b.

[4] W. K. Chow, W. Y. Hung, "Effect of cavity depth on smoke spreading of double-skin façade," Building and Environment, vol. 41, pp. 970-979, 2006.

[5] J. Ji, Y. F. Li, W. X. Shi, J. H. Sun, "Numerical studies on smoke spread in the cavity of a double-skin façade," Journal of Civil Engineering and Management, vol. 22, pp. 470-479, 2016.

[6] L. Miao, C. L. Chow. "A study on window plume from a room fire to the cavity of a double-skin façade," Applied Thermal Engineering, vol. 129, pp. 230-241, 2017.

[7] J. Li, X. Xing, C. Hu, Y. Li, S. Liu, "Numerical studıes on effects of cavıty wıdth on smoke spread ın double-skın façade," Procedia Engineering, vol. 45, pp.695-699, 2012.

[8] G. Thomas, M. Al-Janabi, Donn, M, "Designing double skin facade venting regimes for smoke management," Fire and Materials, vol. 42, pp. 549-560, 2018.

[9] J. Shoa, S. Yeboah, T. Zhu, Y. Li, "Simulation study on the spreading of fire-ınduced smoke in natural-ventilated double-skin facade buildings," in Proceedings of the 11th International Symposium on Heating, Ventilation and

Air Conditioning Singapore, 2019, pp. 1011-1018.

[10] R. Wang, S. He, H. Yue, "Numerical study of smoke spread upon shaft-box type double skin facades," Procedia Engineering, vol. 211, pp. 755-761, 2018.

[11] C. L. Chow, "Full-scale burning tests on double skin façedes fires," Fire and Materials, vol. 37, pp. 17-34, 2013.

[12] W. K. Chow, W. Y. Hung, Y. Gao, G. Zou, H. Dong, "Experimental study on smoke movement leading to glass damages in double-skinned façade," Construction and Building Materials, vol. 21, pp. 556-566, 2007.

[13] A. Vedrtnam, C. Bedon, M. A. Youssef, M. Wamiq, A. Sabsabi, S. Chaturvedi, "Experimental and numerical structural assessment of transparent and tinted glass during fire exposure," Construction and Building Materials, vol. 250, pp. 118918, 2020.

[14] Y. Wang, Y. Zhang, Q Wang, Y. Yang, J. Sun, "The effect of glass panel dimension on the fire response of glass façades," Construction and Building Materials, vol. 181, pp. 588-597, 2018.

[15] Z. Ni, X. Huang, "Experimental and numerical study of fire spread upon double-skin glass facades," in MATEC Web of Conferences 9, Paris, France, 2013, pp. 3009-3019.

[16] C. L. Cheuk, "Spread of smoke and heat along narrow air cavity in double-skin façade fires," Thermal Science, vol. 18, pp. 405-416, 2014.

[17] K. Grewolls, "Computer simulation of fire hazards and evacuation," Fire Toxicity, vol. 12, pp. 607-618, 2010.

[18] K. McGrattan, "Fire Dynamics Simulator-Technical Reference Guide," Washington: NIST, 2006.

[19] NFPA, "NFPA 92: Standard for Smoke Control Systems," Quincy: National Fire Protection Association, 2021.

[20] A. C. Bwalya, M. A. Sultan, N. Benichou, "Design fires for fire safety engineering: a state-of-the-art review," in CIB World Building Congress, Rotterdam, Netherlands, pp. 1-13, 2014.

[21] J. M. Hurley, "SFPE Handbook of Fire Protection Engineering," Fifth Edition New York: Springer, 2016.